



## Letter to the Editor

## Effect of Cr on the creep properties of zirconium alloys

Yang-Il Jung\*, Yong-Nam Seol, Byoung-Kwon Choi, Jeong-Yong Park, Yong-Hwan Jeong

Nuclear Convergence Technology Division, Korea Atomic Energy Research Institute, 1045 Daedeok-dearo, Yuseong, Daejeon 305-353, Republic of Korea

## ARTICLE INFO

## Article history:

Received 19 August 2009

Accepted 22 October 2009

## Keywords:

Zirconium alloys

Creep

Chromium

## ABSTRACT

To investigate the effect of the Cr element in zirconium-based alloys on the creep properties, Zr–1.2Nb–0.1Cr, Zr–1.2Nb–0.5Cr, Zr–1.2Nb–0.3Sn–0.1Cr, and Zr–1.2Nb–0.2Sn–0.3Cr alloys were manufactured and creep tested under a constant stress of 120 MPa at 380 °C for 250 days. As the amount of Cr as well as Sn increased in the studied alloys, the creep strain rates decreased. The strengthening effect of Cr is considered to be efficient when the zirconium alloy contains Nb as an alloying element. The relative contribution of Cr against Sn contents on creep resistance was also observed to be comparable.

© 2009 Elsevier B.V. All rights reserved.

## 1. Introduction

Creep behavior of zirconium alloys has been extensively investigated in the development of nuclear industry, since zirconium is the primary shielding material for nuclear fuel cladding tubes [1–5]. Zircaloy is the foremost commercial zirconium alloy, which contains Sn, Fe, and Cr as main alloying elements. Nowadays, newer alloys such as Zirlo, M5, NDA, and HANA are developed to be applicable to a high burn-up operation. These zirconium alloys tend to include alloying elements of Nb [5–7] and Cu [7] in order to improve corrosion resistance. Most of the alloying elements in zirconium are known to increase the creep resistance by causing solute hardening of the mother alloy.

Sn is a typical solid-solution hardening element that gives rise to low creep strain rates. The size difference between Sn and Zr causes a stress field, and thus affects the dislocation movement and vacancy diffusion during creep. Sn is also known to decrease the stacking fault energy of zirconium [8]. McInteer et al. [9] proposed that the reduced stacking fault energy inhibits the dislocation glide and climb by increasing the width of extended dislocations. Nb is also known to increase creep strength by solid-solution hardening. When the amount of Nb is lower than its solubility limit, the creep rates of Nb-contained zirconium alloys decreased as the Nb contents increased [5,10]. Brenner et al. [11] demonstrated that the creep rates could be reduced (even when the alloy composition was not changed) if the zirconium matrix were saturated with high amounts of Nb.

On the other hand, the effect of Cr, as well as Fe and Cu, on creep resistance has been considered insignificant. Since their solubility in zirconium is very low and these elements are easy to form

second phase precipitates, creep strength improvement by solid-solution hardening is hardly expected. In fact, it was reported that Fe and Cu were less effective than Nb or Sn [12,13]. Kim et al. [12] suggested that high diffusivity of Fe and Cu might mitigate the interaction between their precipitates and moving dislocations. Lee et al. [13] considered Sn to be the major effective element other than Fe and Cr in commercial zirconium alloys. However, we found some experimental evidence that Cr increases the creep resistance of zirconium alloys. The effect of Cr was compared with the Sn contents in this study. The current finding will be able to suggest a new way for the alloy development.

## 2. Experimental procedures

The chemical compositions of the studied zirconium alloys are Zr–1.2Nb–0.1Cr, Zr–1.2Nb–0.5Cr, Zr–1.2Nb–0.3Cr–0.2Sn, and Zr–1.2Nb–0.1Cr–0.3Sn (all wt.%). For each sample preparation, nuclear grade sponge-type Zr was melted with designated alloying elements in an arc melting chamber under an argon atmosphere. The melting was repeated at least three times to homogenize the melted ingots. The melted ingots were solution-treated at 1020 °C for 30 min in a vacuum furnace and then quenched. Hot-rolling was conducted after a pre-heating of 630 °C for 15 min, and cold-rolled three times to obtain a final thickness of 1 mm. Between the cold-rolling steps, the sheets were intermediately annealed at 580 °C in a vacuum furnace for 3 h. The final annealing was varied differently in order to get two distinct microstructures. Partially recrystallized microstructures were obtained by annealing at 510 °C for 3 h, and full recrystallization at 600 °C for 2 h, respectively.

Creep specimens were machined from the sheet along the RD direction with a gauge length and width of 25 mm and 5 mm, respectively. Creep tests were carried out under a constant load

\* Tel.: +82 42 868 8279.

E-mail address: [yijung@kaeri.re.kr](mailto:yijung@kaeri.re.kr) (Y.-I. Jung).

corresponding to a stress of 120 MPa at 380 °C for 250 h. The creep strain was monitored by using a linear variable differential transformer (LVDT) with a 0.001 mm resolution. For the transmission electron microscopy (TEM) observation, the samples were mechanically polished to 70  $\mu\text{m}$  and then jet-polished with a 90C<sub>2</sub>H<sub>5</sub>OH–10HClO<sub>4</sub> (vol.%) solution under –45 °C and 15 V conditions. The microstructures, including the second phase particles of the samples, were analyzed by using a TEM equipped with an energy dispersive X-ray spectroscopy (EDS).

### 3. Results and discussion

Fig. 1 shows the variation in creep strain of the studied zirconium alloys. All the samples showed both a primary and a secondary (steady state) creep behavior during 250 h, as shown in Fig. 1. As the total amount of alloying elements increased, the creep deformations were reduced. Zr–1.2Nb–0.1Cr exhibited the highest creep rate, and Zr–1.2Nb–0.5Cr showed the lowest creep rate. In the case of Zr–1.2Nb–(0.2–0.3)Sn, the sample containing 0.3Cr revealed a lower creep rate than that containing 0.1Cr. The effect of Sn can be deduced from the Zr–1.2Nb–0.1Cr and Zr–1.2Nb–0.1Cr–0.3Sn samples; the addition of Sn decreased the strain rate by a half to a third. These results are very apparent in the case of fully recrystallized samples. Since the creep is a plastic deformation process accompanied by the movement of dislocations, complete recrystallization (absence of dislocations) results in slow creep

strain rates. According to Fig. 1, partially recrystallized samples (Fig. 1a) represented more than 1.5 times faster creep rates than fully recrystallized samples (Fig. 1b).

Since entangled dislocations could be a barrier for the dislocation movement for the creep, it is expected that cold-worked or partially recrystallized samples exhibit the lower creep rates than fully recrystallized samples. At high stress level, the above work-hardening mechanism operates; however, the high dislocation density appears to allow more creep strain at low stress level ( $\leq 120$  MPa). The obtained lower creep rates in fully recrystallized samples (as shown in Fig. 1) were consistent with previous works in Zr-based alloys [14–16]. In addition, the primary creep was noticeable when the initial dislocation density was high. The saturated primary creep strains ( $\epsilon_{\text{sat}}$ ) and secondary creep rates ( $\dot{\epsilon}_{\text{ss}}$ ) are presented in Table 1. Saturated primary creep strain was determined from the extrapolation of secondary creep rate ( $\dot{\epsilon}_{\text{ss}}$ ) down to zero exposure time.

The creep rates can be affected by the initial dislocation densities in the samples. The initial dislocation densities in the partially recrystallized samples (Fig. 1a) must be different among samples, because the degree of recrystallization would be varied depending on the chemical composition of the alloy [17]. Therefore, the creep test results using partially recrystallized samples might induce an adverse conclusion. However, the observed identical results irrespective of the samples' microstructures suggest the positive effect of Cr as well as Sn on the improvement of the creep strength.

Fig. 2 demonstrates the TEM micrographs of the crept specimens for the recrystallized samples. Dislocations were formed in the crept grains, which indicate the creep proceeded with the dislocation glide and climb process in the current experimental conditions. According to the EDS analysis as shown in Table 2, the second phase particles containing Cr was not observed essentially in the Zr–1.2Nb–0.1Cr alloy. Most of the second phase particles consisted of Zr, Nb, and Fe. The iron detection in the precipitates was caused by an iron impurity in the sponge-type Zr. Since the solubility of Fe is very low (about several ppm), the presence of iron in the second phase particles is reasonable. However, the absence of Cr in the precipitates is a concern, since the solubility of Cr is also known to be as low as that of Fe [18]. (Even though the detection resolution for the elemental analysis in this study is very poor, the Cr precipitates should be presented in all samples.) The solubility studies on Cr in zirconium had been based on the Zircaloy system (without Nb elements). The solubility can be varied depending on the co-existing elements in the multi-component alloy systems. The high Cr solubility of 1 at.% was reported in Zr–Cr–O system [19]. Moreover, the Zr–xNb second phase particles can accommodate a portion of Cr contents when zirconium alloys contain Nb [20]. According to our results, the Zr–1.2Nb binary system is supposed to increase the Cr solubility up to at least 0.1 wt.%. In addition, the increased creep resistance with Cr addition up to 0.5 wt.% suggests that a particle hardening can operate as well.

According to Fig. 1, the addition of Cr reduced the secondary creep strain rates from  $2.9 \times 10^{-8} \text{ s}^{-1}$  to  $5.2 \times 10^{-9} \text{ s}^{-1}$  when Cr was increased from 0.1 wt.% to 0.5 wt.% in the case of Zr–1.2Nb, and from  $1.1 \times 10^{-8} \text{ s}^{-1}$  to  $8.0 \times 10^{-9} \text{ s}^{-1}$  when Cr was increased

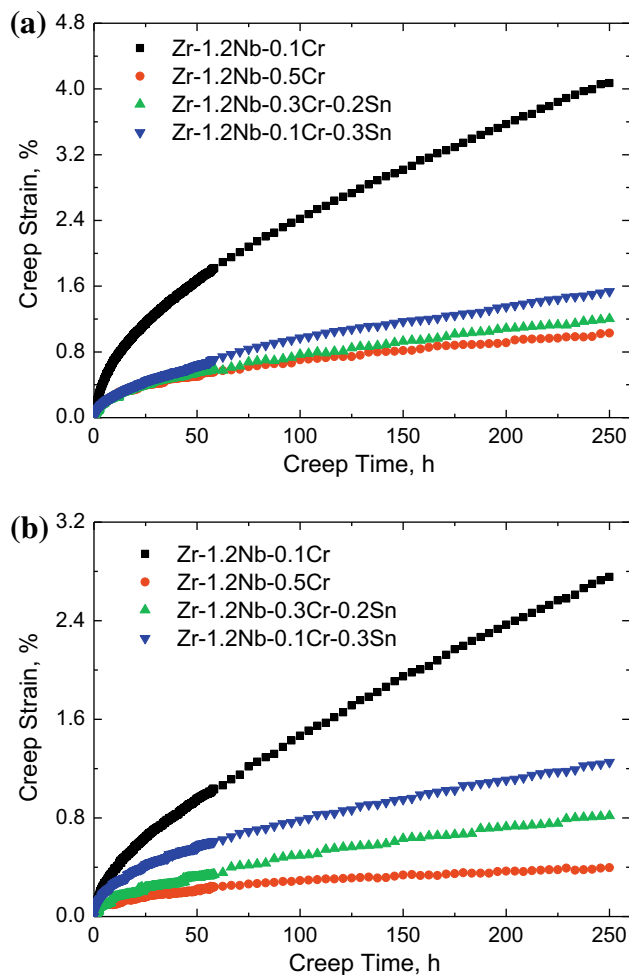


Fig. 1. Variations in the creep strains of the Zr–Nb–Sn–Cr alloys with having: (a) partially recrystallized microstructures and (b) fully recrystallized microstructures under a constant stress of 120 MPa at 380 °C.

Table 1

Saturated primary creep strains ( $\epsilon_{\text{sat}}$ ) and secondary creep rates ( $\dot{\epsilon}_{\text{ss}}$ ) for partially recrystallized (PRx) and fully recrystallized (Rx) samples.

Alloys	$\epsilon_{\text{sat}}$ (%)		$\dot{\epsilon}_{\text{ss}}$ ( $\times 10^{-8} \text{ s}^{-1}$ )	
	PRx	Rx	PRx	Rx
Zr–1.2Nb–0.1Cr	1.5	0.8	2.94	2.27
Zr–1.2Nb–0.1Cr–0.3Sn	0.7	0.5	1.08	0.80
Zr–1.2Nb–0.3Cr–0.2Sn	0.6	0.3	0.80	0.55
Zr–1.2Nb–0.5Cr	0.5	0.2	0.52	0.21

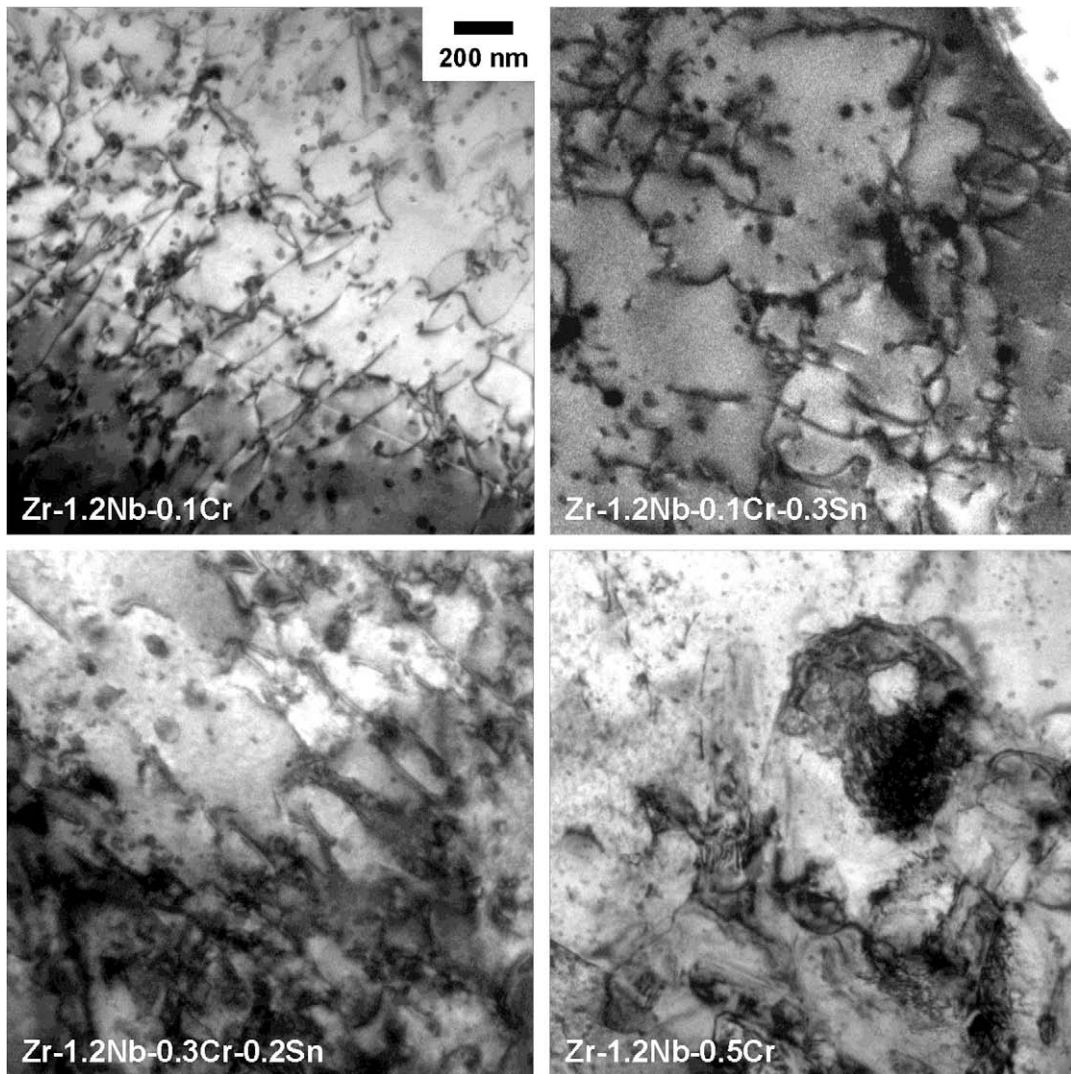


Fig. 2. TEM microstructures of the crept zirconium alloy specimens showing the formed dislocations during creep under 120 MPa at 380 °C for 250 h.

Table 2

Average chemical compositions of the observed second phase particles.

Alloys	Nb (at.%)	Cr (at.%)	Fe (at.%)	Zr (at.%)
Zr-1.2Nb-0.1Cr	19.47	<0.10 <sup>a</sup>	0.23	78.18
Zr-1.2Nb-0.1Cr-0.3Sn	24.25	1.11	0.28	74.35
Zr-1.2Nb-0.3Cr-0.2Sn	28.81	3.60	0.89	63.92
Zr-1.2Nb-0.5Cr	19.24	3.22	0.13	79.82

<sup>a</sup> Lower than the confidence limit of detection of the EDS analysis.

from 0.1 wt.% to 0.3 wt.% in the case of Zr-1.2Nb-(0.2–0.3)Sn, respectively. If the amount of Cr and Sn were considered as a single parameter, the best correlation between that amount and the creep rates could be presented as shown in Fig. 3. The relative effect of Cr is slightly higher than that of Sn. The coefficient (weight factor) of Cr to Sn was assumed to be 1.2 for this study. For the best linear fit of the graphs shown in Fig. 3, the weight factor was found to be 1.4 for partial recrystallized samples and 2.0 for full recrystallized samples by using the least square method.<sup>1</sup> Previously, Pahutová

<sup>1</sup> For the determination of the weight factor,  $w$ , the alloying amount of Sn and Cr was considered as a variable,  $X (= Sn + w \times Cr)$ , and its corresponding secondary creep rate was treated as a co-variable,  $Y$ . The value that minimizes the sum of squared residuals of the linear regression of the  $X$ - $Y$  function was calculated as the optimum weight factor.

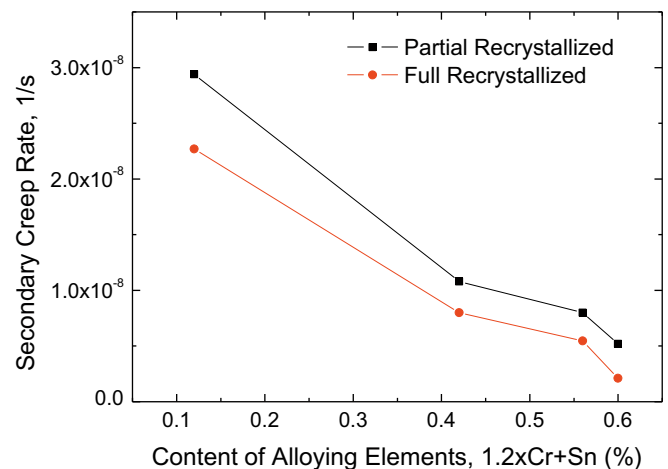


Fig. 3. Correlation between the steady state creep strain rates and the amount of alloying elements Cr and Sn. It is assumed that Cr has a weight factor of 1.2 times than that of Sn.

et al. [10] reported excellent creep resistance of Mo containing zirconium alloys. They suggested the solute atom atmosphere caused by

atomic radius difference was strong in the case of Mo. The atomic size difference for Mo is about 13%, in contrast to about 3% for Sn and 9% for Nb. Since the size difference is about 20% in the case of Cr, the creep resistance will be better by forming a strong solute atmosphere.

Sn is known to increase creep strength of zirconium alloys, and thus considered the most typical alloying element [8,9,13]. On the other hand, Sn is also known to degrade the corrosion resistance. Thus, newer alloys are containing Nb to enhance the corrosion properties of Sn containing Zircaloy cladding tubes. Since Cr is not harmful to the corrosion resistance, the synergic effect of Cr on creep and corrosion properties is expected. The enhanced creep resistance by the Cr addition in zirconium alloys would be possible when the alloys contained a few percent of Nb, although the definite hardening mechanism is unclear yet. In order to get the high corrosion resistance and high creep strength, it is desirable to add Cr and Nb elements and to decrease Sn contents in Zircaloy based alloys.

#### 4. Conclusion

The effect of the Cr element in zirconium-based alloys on the creep properties was investigated. Even though the solubility of Cr in zirconium is very limited, an improvement in the creep resistance was noted. The addition of Cr exhibited creep strengthening with an effect comparable to that of the addition of Sn contents. Therefore, a way for the zirconium alloy development can be suggested in this study, i.e. Cr and Nb addition along with Sn reduction among the alloying elements.

#### Acknowledgements

This study was supported by the Korean Government's Ministry of Education, Science and Technology (MEST), through its Nuclear R&D Program. And authors thank Mr. H.-D. Cho and Ms. S.M. Shin for the TEM operation (JEM-2010, 200 kV, at KAERI and JEM-3010, 300 kV, at KAIST).

#### References

- [1] D.G. Franklin, G.E. Lucas, A.L. Bement, Creep of Zirconium Alloys in Nuclear Reactors, ASTM STP 815, Philadelphia, 1983.
- [2] V. Fidleris, J. Nucl. Mater. 159 (1988) 22–42.
- [3] K.L. Murty, G. Dentel, J. Britt, Mater. Sci. Eng. A 410–411 (2005) 28–31.
- [4] T.A. Hayes, M.E. Kassner, Metal. Mater. Trans. A 37A (2006) 2389–2396.
- [5] I. Charit, K.L. Murty, J. Nucl. Mater. 374 (2008) 354–363.
- [6] J.-P. Mardon, D. Charquet, J. Senevat, ASTM STP 1354, 2000, pp. 505–524.
- [7] Y.H. Jeong, S.-Y. Park, M.-H. Lee, B.-K. Choi, J.-H. Baek, J.-Y. Park, J.-H. Kim, H.-G. Kim, J. Nucl. Sci. Technol. 43 (2006) 977–983.
- [8] D.H. Sastry, M.J. Luton, J.J. Jonas, Philos. Mag. 30 (1974) 115–127.
- [9] W.A. McInteer, D.L. Baty, K.O. Stein, ASTM STP 1023, 1989, pp. 621–640.
- [10] M. Pahutová, K. Kuchařová, J. Čadek, Mater. Sci. Eng. 27 (1977) 239–248.
- [11] R. Brenner, J.L. Béchade, O. Castelnu, B. Bacroix, J. Nucl. Mater. 305 (2002) 175–186.
- [12] H.-G. Kim, Y.-H. Kim, B.-K. Choi, Y.-H. Jeong, J. Nucl. Mater. 359 (2006) 268–273.
- [13] S.Y. Lee, K.T. Kim, S.I. Hong, J. Nucl. Mater. 392 (2009) 63–69.
- [14] H. Stehle, E. Steinberg, E. Teckhoff, ASTM STP 633, 1977, pp. 486–507.
- [15] D. Gilbon, A. Soniak, S. Doriot, J.P. Marson, ASTM STP 1354, 2000, pp. 51–73.
- [16] C. Nam, B.-K. Choi, M.-H. Lee, Y.-H. Jeong, J. Nucl. Mater. 305 (2002) 70–76.
- [17] Y.-I. Jung, M.-H. Lee, H.-G. Kim, J.-Y. Park, Y.-H. Jeong, J. Alloy. Compd. 479 (2009) 423–426.
- [18] M. Canay, C.A. Danón, D. Arias, J. Nucl. Mater. 280 (2000) 365–371.
- [19] R.O. González, L.M. Gribaudo, J. Nucl. Mater. 342 (2005) 14–19.
- [20] W.-Y. Kim, T. Takasugi, Scripta Mater. 48 (2003) 559–563.